

Fault Tolerance of Semiactive Seismic Isolation

Henri Gavin, A.M.ASCE;¹ Cenk Alhan, S.M.ASCE;² and Natasha Oka³

Abstract: A six-story seismically isolated structure fitted with semiactive hydraulic devices is analyzed in order to study the effect of time lag in the devices and mass eccentricity in the superstructure on the lateral-torsional behavior. The computer program *3DBASIS*, which allows the nonlinear dynamic analysis of three-dimensional structures, is used in this work. Appropriate modifications were made to this program to incorporate the behavior of semiactive hydraulic devices. Three different types of base isolation systems were considered: (1) lead rubber bearings; (2) lead rubber bearings with supplemental viscous damping; and (3) lead rubber bearings with semiactive viscous damping. A comparison of these three base-isolation systems, considering both the effects of eccentricity in the structure and differential time lags in semiactive hydraulic devices are studied. The peak isolator shear, isolation drift, rotation, and torsional moment are reported. Three major earthquake motion records, namely, the El Centro record of the 1940 Imperial Valley earthquake, the Meloland record of the 1979 Imperial Valley earthquake, and the Sylmar free field record of the 1994 Northridge earthquake were used as inputs in the analyses.

DOI: 10.1061/(ASCE)0733-9445(2003)129:7(922)

CE Database subject headings: Seismic isolation; Base isolation; Damping; Vibration control; Earthquake engineering.

Introduction

Seismic isolation is a successful method for protecting structures from earthquakes. The basic objectives in the seismic isolation of building structures are to protect structural integrity and to prevent injury to the occupants and damage to the contents (Skinner et al. 1993; Housner et al. 1997; Kelly 1997; Meirovitch and Stemple 1997; Naeim and Kelly 1999). The compliant elastomeric bearings and frictional sliding mechanisms installed in the foundations of seismically isolated structures protect these structures from strong earthquakes through a reduction of stiffness and an increase in damping. The reduction of stiffness is intended to detune the structure's fundamental period from the characteristic period of earthquake ground motions. Isolation bearings are designed to accommodate large displacement demands and to mobilize damping mechanisms, typically through material yielding of a lead column within the isolator. Elastomeric bearings are made by vulcanizing sheets of rubber to thin steel reinforcing plates, and are stiff in the vertical direction and flexible in the horizontal direction (Kelly 1997; Naeim and Kelly 1999). Because of this, under seismic loading the bearing system isolates the building from the horizontal components of the ground movement. Friction pendulum bearings (Tyler 1977) for seismic isolation also entail highly nonlinear dynamic behavior and were ana-

lyzed with an efficient model by Wang et al. (1998). An experimental study was performed to evaluate the feasibility of a sliding isolation system equipped with uplift restraint devices for medium rise buildings subject to column uplift (Nagarajaiah et al. 1992).

Base-isolation systems are being implemented in an increasing number of projects in highly seismic areas throughout the world (Hussain and Retamal 1994). The first base-isolated building in the United States was the Foothill Communities Law and Justice Center in San Bernardino County, California in 1986 (Kelly 1991). More recent examples of seismically isolated buildings include the University of Southern California USC University Hospital in Los Angeles, the Emergency Operations Center in Los Angeles, the U.S. Court of Appeals in San Francisco, and the San Bernardino County Medical Center (EERC 2001). Some examples of buildings constructed using rubber bearing isolation systems are the Salt Lake City and County building, the Rockwell International Headquarters in Seal Beach, CA, the Long Beach Hospital in Long Beach, CA, the State of California Justice Building in San Francisco, and the Government Office Building in Wellington, New Zealand.

During the 1994 Northridge earthquake, the seismic isolation system of the USC Hospital building reduced the structural response when compared to an equivalent fixed-base structure (Nagarajaiah and Xiaohong 2000). The bearings yielded and dissipated energy and the superstructure remained elastic, as intended. Experiments on two four-story buildings, one supported on high-damping rubber isolation and the other on a fixed-base, were conducted by Moroni et al. (1998). For the 24 earthquake records evaluated, the reduction in the maximum acceleration at the roof level for the isolated building, as compared to the fixed-base one, varied from 1 to 3.5, depending on the level of maximum ground acceleration and the characteristics of the earthquake motions. Other base-isolated structures behaved as designed during the 1994 Northridge and 1995 Kobe earthquakes (Kelly 1991, DIS 2001). On the other hand, protection of seismically isolated structures from strong, long-period velocity pulses can be much more

¹Associate Professor, Dept. of Civil Engineering, Duke Univ., Durham, NC 27708-0287. E-mail: hpgavin@duke.edu

²Graduate Assistant, Dept. of Civil Engineering, Duke Univ., Durham, NC 27708-0287.

³Graduate Assistant, Dept. of Civil Engineering, Duke Univ., NC 27708-0287.

Note. Associate Editor: Takeru Igusa. Discussion open until December 1, 2003. Separate discussions must be submitted for individual papers. To extend the closing date by one month, a written request must be filed with the ASCE Managing Editor. The manuscript for this paper was submitted for review and possible publication on July 10, 2001; approved on March 6, 2002. This paper is part of the *Journal of Structural Engineering*, Vol. 129, No. 7, July 1, 2003. ©ASCE, ISSN 0733-9445/2003/7-922-932/\$18.00.

challenging. A study by Heaton et al. (1995) showed that a base-isolated building subjected to a near-field M_w 7.0 blind thrust earthquake could result in large isolator drifts (in excess of 50 cm) even when damped at 25% critical damping. Large displacements at the isolation interface during a strong earthquake can lead to buckling or rupture of the isolation bearings (Nagarajaiah and Ferrell 1999). Although, large levels of damping reduce isolator displacements in the fundamental mode, they impart forces into the structure which can increase structural accelerations and deformations in higher modes, and can increase interstory displacements (Kelly 1999). To address the need for high damping to limit the isolation drift and low damping to improve the isolation effectiveness at high frequencies, multiple controllable damping (semiactive) systems have been proposed (Carlson and Spencer 1996, Symans and Constantinou 1997a, b, Johnson et al. 1998, Patten et al. 1998, Gavin and Doke 1999; Symans and Constantinou 1999, Yang et al. 2000). Semiactive control systems were first proposed in the 1920s, as shock absorbers which utilized an elastically supported mass to activate hydraulic valving. Neither external power nor a solenoid valve were necessary to direct the hydraulic flow within the damper (Karnopp et al. 1974, 1975). By definition (Spencer and Sain 1997), semiactive control systems are implemented using devices which cannot increase the mechanical energy of the system. Devices with controllable damping and stiffness properties are typically used in the implementation of semiactive control systems. These devices can be used to approximate the actions of force and power-generating actuators, but do not require large external power sources. Furthermore, because of the energy-dissipation properties of semiactive devices, the control system is unconditionally stable in a bounded-input, bounded-output sense. Semiactive control systems provide the robustness of passive control systems and the performance of active control systems (Symans and Constantinou 1999).

Semiactive devices can be categorized as follows (Kurata 1999).

1. **Controllable fluid damper:** These encompass devices which utilize electrorheological or magnetorheological materials (Ehrgott and Masri 1993; Makris, Hills, Burton, and Jordan 1995; Carlson and Spencer 1996; Gavin et al. 1996, Spencer, Dyke, and Sain 1996). These materials have the ability to change from free flowing viscous fluids to a semisolid state in a matter of milliseconds when exposed to electric or magnetic fields. These devices are able to regulate forces without an electromechanical mechanism;
2. **Controllable friction damper:** These dampers utilize the force generated by surface friction to dissipate energy. Dowdell and Cherry (1994) proposed a variable slip force friction damper and an "ON-OFF" friction damper. Hirai, Naruse, and Abiru (1996) investigated a variable friction damper utilizing piezoelectric actuators. Akbay and Aktan (1990) proposed a friction slip brace. A study by Feng (1993) investigates into a hybrid isolation system—a frictional controllable sliding system. This hybrid system was developed using friction controllable bearings. It is shown that this type of system is effective for earthquakes with a broad range of intensity, compared to its conventional passive counterparts;
3. **Hydraulic damper:** Fluid viscous dampers have found numerous applications in the shock vibration isolation of aerospace and defense systems. The earliest well documented use of large fluid dampers was by the military to reduce the recoil of large canons. Karnopp et al. (1974) introduced semiactive isolators using the skyhook damper scheme. Practical applications of skyhook dampers, namely, extreme

isolation for delicate manufacturing operations against seismic input and the automotive suspensions are discussed by Karnopp (1990) researcher. Patten, Mo, Kuehn and Lee (1998), provided a primer on the important physical characteristics of a hydraulic semiactive vibration absorber. An important benefit of the fluid viscous dampers is that they are especially effective in minimizing the forces acting on building columns. They reduce the drifts and shear forces which are in phase with column bending moments.

The development and evaluation of semiactive control systems for applications to structural control is receiving particular attention (Symans and Constantinou 1999). Numerical simulations, vibration tests, and semiactive vibration suppression experiments of a ten bay truss bridge with ER fluid dampers were performed by Onoda et al. (1997). Gavin and Hanson (1998) showed that adaptive base-isolation systems using electrorheological materials in viscous damping walls can reduce absolute velocities in upper stories as well as deflections in the isolation system. Seismic testing of a multistory building structure with a semiactive fluid damper control system was performed by Symans and Constantinou (1997a). The semiactive dampers were installed in the lateral bracing of the structure and the mechanical properties of the dampers were modified according to control algorithms which utilized the measured response of the structure. An intelligent base-isolation system, comprised of low-damping isolation bearings and controllable fluid dampers was studied by Johnson et al. (1998). In another study, Symans and Constantinou (1997b) discussed the development, experimental testing, and analytical modeling of an intelligent seismic control system. These studies demonstrate the potential of semiactive damping systems, but do not consider the possibility of asymmetry in the buildings or relative time lag between the semiactive devices. While many previous studies have shown the benefits of semiactive control in planar structures, the possibility of mistimed devices due to technical problems may result in high-torsional response. This increase in high-torsional response is typically compounded by the effects of significant mass eccentricity. Very few analytical studies have been reported on the seismic isolation of three-dimensional (3D) building models (Jangid and Datta 1995). Lee (1980) has shown that base isolation reduces the structural torsion even if the structural eccentricity is large. Pan and Kelly (1983) studied the effect of eccentricity on the elastic response of a rigid mass supported on a base isolator. Nagarajaiah et al. (1991, 1993) studied the response of a 3D base-isolated building with biaxial hysteretic isolators. Jangid and Datta (1992, 1993, 1994, 1995) conducted parametric studies on the response behavior of a torsionally coupled base-isolation system. Additionally, it is widely recognized that time lags exist in active control systems and must be considered to ensure dynamic stability (McGreevy et al. 1988; Soong 1990; Symans and Constantinou 1997a).

In this paper, the effects of time lag in the semiactive devices and the eccentricity in the mass of the superstructure are studied. A comparison between three base-isolation systems is presented: (1) lead rubber bearings (LRB); (2) lead rubber bearings with supplemental viscous damping (LRB-VD); and (3) lead rubber bearings with semiactive viscous damping (LRB-SAVD). Three earthquake motion records, namely, the El Centro record of the 1940 Imperial Valley earthquake, the Meloland record of the 1979 Imperial Valley earthquake, and the Sylmar free field record of the 1994 Northridge earthquake, were used as inputs in the analyses. The El Centro record is selected as a moderate earthquake,

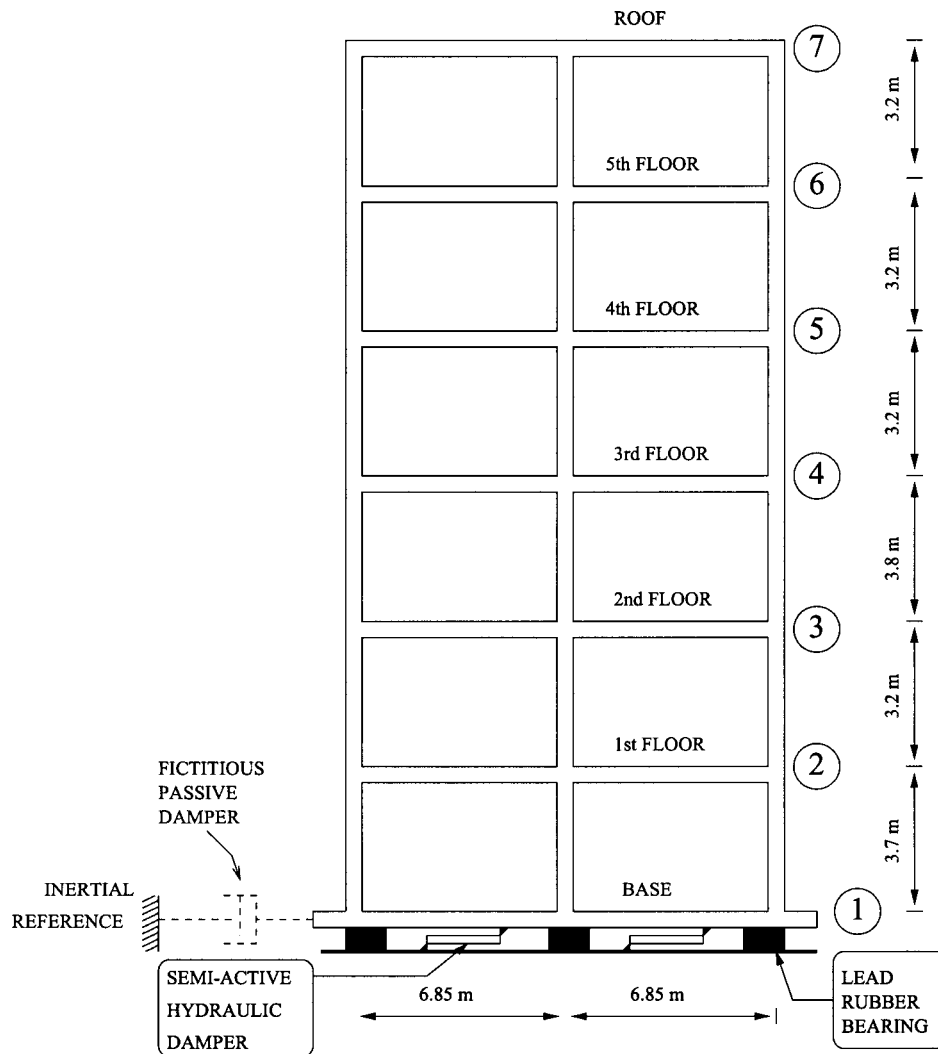


Fig. 1. Base isolated structure with controllable hydraulic devices

while Meloland and Sylmar records are representative of pulse-like earthquake ground motions. This study addresses the robustness of semiactive base isolation systems with respect to relative time lags among the devices.

Control Rule Development and Device Placement

Consider a base-isolated building with controllable hydraulic devices as shown in Fig. 1. The displacement z is the displacement of the ground with respect to an inertial reference frame. The displacements of the degrees of freedom with respect to the ground are x_1, \dots, x_7 . The control objective is to suppress the absolute motion of the building and to thereby reduce the dynamic shear forces carried by the structure. Ideally, this can be achieved by means of a fictitious passive damper which imparts a force to the building foundation proportional to the absolute velocity of the base ($\dot{z} + \dot{x}_1$) as illustrated in Fig. 1. The behavior of this fictitious damper can be mimicked by a semiactive control device placed as shown in Fig. 1. The device will have high damping (ON) when the force in the device has the same sign as the velocity ($\dot{x}_1 + \dot{z}$) and will have low damping (OFF) otherwise (Karnopp et al. 1974).

An autonomous vibratory system is stable if its total internal energy $V(t)$ decreases monotonically toward a state of static equilibrium. This basic fact motivates Lyapunov's direct method, which states that the internal energy of a system with an asymptotically stable equilibrium state decays monotonically in time toward the energy of the equilibrium state. An attractive feature of this method is that the sign of $V(t)$ and its derivative $\dot{V}(t)$ give information regarding the equilibrium, and the exact value of $V(t)$ is not always needed (Khalil 1996).

This physically motivated control strategy can be mathematically derived as follows. The equations of motion of a base excited structure are given by

$$\mathbf{M}(\ddot{\mathbf{x}} + \mathbf{H}\ddot{\mathbf{z}}) + \mathbf{r}(\mathbf{x}, \dot{\mathbf{x}}) + \sum_{n=1}^N \mathbf{b}_n f_n(\mathbf{b}_n^T \mathbf{x}, \mathbf{b}_n^T \dot{\mathbf{x}}, u_n) = 0 \quad (1)$$

where \mathbf{x} contains the displacements of the structure relative to ground; \mathbf{b}_n =control input vector and depends on the placement of the n th device; \mathbf{H} =boolean earthquake input matrix; $\ddot{\mathbf{z}}$ =two orthogonal components of horizontal ground acceleration; $\mathbf{r}(\mathbf{x}, \dot{\mathbf{x}})$ =generalized nonlinear restoring forces; \mathbf{M} =positive definite mass matrix; f_n =force in the device; N =total number of devices; and u_n =control input.

The total energy of the system is given by

$$V(t) = W(\mathbf{x}, \dot{\mathbf{x}}) + \frac{1}{2} (\dot{\mathbf{x}} + \mathbf{H}\dot{\mathbf{z}})^T \mathbf{M} (\dot{\mathbf{x}} + \mathbf{H}\dot{\mathbf{z}}) \quad (2)$$

where $\frac{1}{2}(\dot{\mathbf{x}} + \mathbf{H}\dot{\mathbf{z}})^T \mathbf{M} (\dot{\mathbf{x}} + \mathbf{H}\dot{\mathbf{z}})$ = total kinetic energy of the system; $\dot{\mathbf{z}}$ = ground velocity; and $\mathbf{r}(\mathbf{x}, \dot{\mathbf{x}})$ = gradient of the potential energy function $W(\mathbf{x}, \dot{\mathbf{x}})$. We choose the total kinetic energy in this formulation to stabilize the structure with respect to an inertial frame of reference. Choosing the kinetic energy with respect to the ground motion results in a Lyapunov control rule which maximizes the damping and stiffness of the structure. While the deformations of stiff and highly damped structures will be small, the total accelerations can be high. The intent of Eq. (2) is to apply damping in a way that decreases the absolute motion of the structure. Because the control forces are introduced through isolation damping, as shown in Fig. 1, the deformation of the isolators are also suppressed. Following Lyapunov's direct method, the objective of the control is to minimize the internal energy by forcing the internal energy to decrease as quickly as possible. The rate of change of the internal energy is

$$\dot{V}(t) = -\dot{\mathbf{x}}^T \mathbf{r} - \dot{\mathbf{z}}^T \mathbf{H}^T \mathbf{r} - \sum_{n=1}^N [(\dot{\mathbf{x}} + \mathbf{H}\dot{\mathbf{z}})^T \mathbf{b}_n f_n(\mathbf{b}_n^T \mathbf{x}, \mathbf{b}_n^T \dot{\mathbf{x}}, \mathbf{u}_n)] \quad (3)$$

The only terms that can be controlled in Eq. (3) are the terms in square brackets. In order to make $V(t)$ decrease as quickly as possible, a device's force should be made large whenever the quantity in the square bracket is positive, otherwise the device force should be small. The vectors \mathbf{b}_n define the placement of the devices. For a device connecting degrees of freedom "i" to the base, $b_i = 1$ and all other elements of \mathbf{b} are zero. If the device connects degree of freedom "i" with the degree of freedom "j," then $b_i = 1$, $b_j = -1$, and all other elements of \mathbf{b} are zero. Also note that any controllable damping device unconditionally satisfies the same sector-bounded passivity constraints as any damper: $\mathbf{b}^T \dot{\mathbf{x}} f(\mathbf{b}^T \mathbf{x}, \mathbf{b}^T \dot{\mathbf{x}}) > 0$. Therefore, if $b_{i,j} = \pm 1$ then

$$(\dot{\mathbf{x}} + \mathbf{H}\dot{\mathbf{z}})^T \mathbf{b} = \dot{x}_i - \dot{x}_j = \mathbf{b}^T \dot{\mathbf{x}} \quad (4)$$

and if $b_i = 1$ only

$$(\dot{\mathbf{x}} + \mathbf{H}\dot{\mathbf{z}})^T \mathbf{b} = \dot{x}_i + \dot{z} \neq \mathbf{b}^T \dot{\mathbf{x}} \quad (5)$$

Therefore, if one end of the device is not attached to the moving ground, the term in the square brackets is always positive. Such a device placement requires the device to be "ON" always, which defeats the very purpose of a controllable device. Thus, for this particular control rule, the controllable device is placed between the foundation and the ground (Gavin and Doke 1999; Gavin 2001). The control rule reduces to turning the n th semi-active device "ON" to maximize its damping when $f \cdot V_a > 0$, where V_a is the absolute velocity of the structure-side of the device. The control decision is based only on the signs of the motion and the force of the device and no centralized control computation is needed.

Online Integration of Acceleration

The integrator shown in Fig. 2 is tuned to integrate frequencies at the fundamental mode of the isolated structure with no phase lag (Gavin et al. 1998; Gavin 2001). Figs. 3(a and b) show the Bode magnitude and phase of the integrator. The integrator suppresses low-frequency bias and drift errors as well as high-frequency noise. To evaluate the accuracy of the on-line velocity estimation,

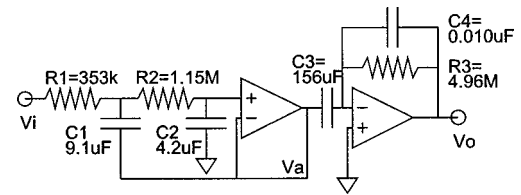


Fig. 2. Analog integrator, tuned for base isolated building frame

ground velocities were also precomputed through a frequency-domain integration of the ground acceleration records, between frequencies of 0.05 and 20 Hz, and were added to the simulated base velocity relative to the ground. Figs. 3(c and d) illustrate the base velocity computed by summing precomputed ground velocities with simulated relative base velocities (dashed) and the output of the on-line integration of the measured absolute acceleration of the base (solid). Fig. 3(d) shows that the hysteresis of the on-line integrator is small and that the sign of the velocity, which is essentially all that the control rule requires, may be accurately estimated on-line with this simple circuit. The ordinary differential equations for this circuit may also be simulated with digital signal processing hardware, although this is not necessary. This example is for the 1940 El Centro earthquake record. The integrator performs better with long-period pulse-like ground motion

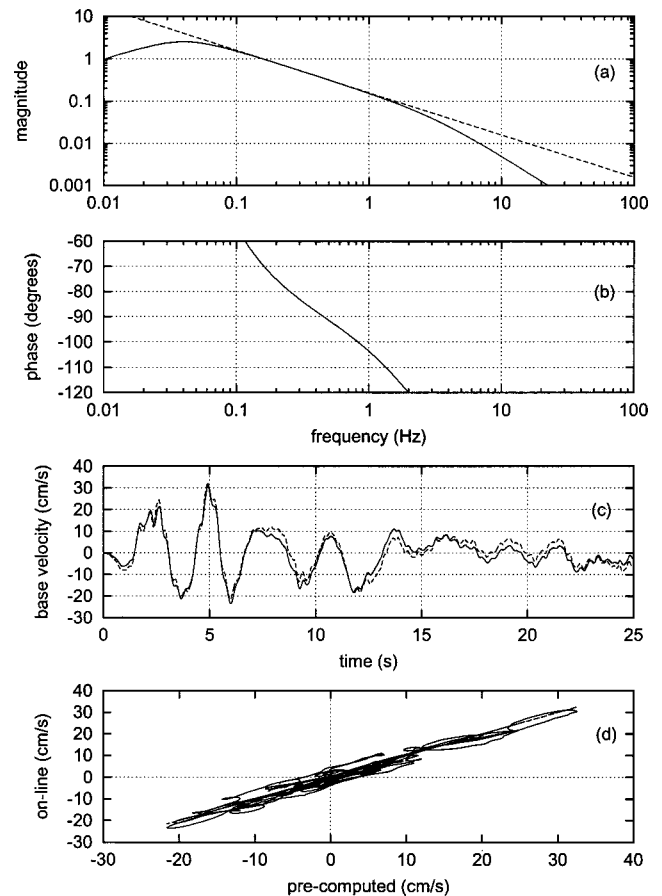


Fig. 3. Performance of on-line base velocity computation: (a) bode magnitude and (b) bode phase of integrator; (c) on-line (solid) and a-causal (dashed) computation of base velocity; and (d) hysteresis of on-line base velocity estimation for El Centro (1940) ground accelerations

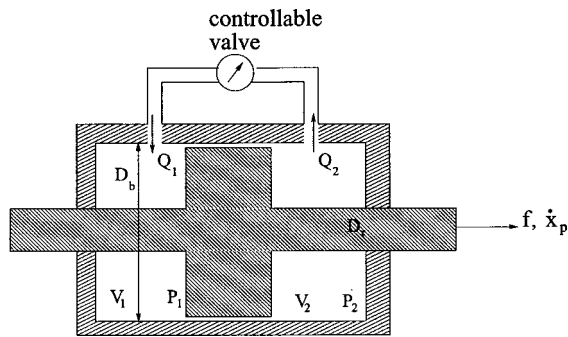


Fig. 4. Details of hydraulic device

records (i.e., Northridge-Sylmar and Kobe) because these records do not excite the higher modes of isolated structures as significantly.

Design and Modeling of Semiactive Hydraulic Device

The controllable damping device modeled in this study comprises a hydraulic cylinder with a controllable by-pass valve and can be fashioned from a conventional damper with provision for fast modulation of the damping coefficient. The device is termed “semiactive,” because the power required to perform the necessary modulation in forces is generated by the motion of the structure itself.

Consider a fluidic device as shown in Fig. 4. The control device illustrated here essentially consists of a hydraulic cylinder, a piston, and a valve. The flow of fluid is controlled by means of a valve, with a variable valve coefficient $c_v^*(v)$, where v is the valve opening variable. The area of the piston is A_p , the pressure differential across the two chambers is $p_2 - p_1$, and the device contains a volume of fluid V_T where $V_T = V_1 + V_2$. The diameter of the bore and that of the rod are D_b and D_r , respectively. Through equilibrium, the force f in the piston rod is $A_p(p_2$

$-p_1)$. Assuming incompressible flow in the value $Q_1 = Q_2 = Q$ and approximating a linear pressure-flow relationship for the controllable value $(p_2 - p_1) = c_v^*(v)Q$, where $c_v^*(v)$ has units of $[N s/m^5]$. Considering fluid compressibility within Chambers 1 and 2, $\dot{p}_1 V_1 = -\beta \dot{V}_1$ and $\dot{p}_2 V_2 = -\beta \dot{V}_2$, where β is the bulk modulus of the hydraulic fluid which can range from 80 to 200 kN/cm² and where we apply the conventions that $\dot{V} > 0$ means volumetric expansion and $\dot{p} > 0$ means increasing hydrostatic compression. In Chamber 1, $\dot{V}_1 = -Q_1 + A_p \dot{x}_p$ and in Chamber 2, $\dot{V}_2 = Q_2 - A_p \dot{x}_p$. Combining the pressure-flow relationship, the equilibrium equation and the compressibility equations with the approximation that flow in the valve is incompressible, we obtain

$$\dot{p}_2 = -\frac{\beta}{V_2} \frac{f}{A_p c_v^*(v)} + \frac{\beta}{V_2} A_p \dot{x}_p \quad (6)$$

and

$$-\dot{p}_1 = -\frac{\beta}{V_1} \frac{f}{A_p c_v^*(v)} + \frac{\beta}{V_1} A_p \dot{x}_p \quad (7)$$

Details of these derivations are found in Patten et al. (1998) and Gavin and Doke (1999). Adding Eqs. (6) and (7)

$$\dot{p}_2 - \dot{p}_1 = -\frac{\beta}{A_p c_v^*(v)} \left(\frac{1}{V_1} + \frac{1}{V_2} \right) f + \beta A_p \left(\frac{1}{V_1} + \frac{1}{V_2} \right) \dot{x}_p \quad (8)$$

and the equation for the damper force, including compressibility and viscous effects is linearized as

$$\dot{f} = -\frac{k_d}{c_v(v)} f + k_d \dot{x}_p \quad (9)$$

where

$$k_d = \frac{4\beta A_p^2}{V_T} \quad (10)$$

is the hydraulic stiffness of the device at midstroke. Considering elastic properties of the built-up device, the overall device stiffness k_d is less than the hydraulic stiffness. The device valve con-

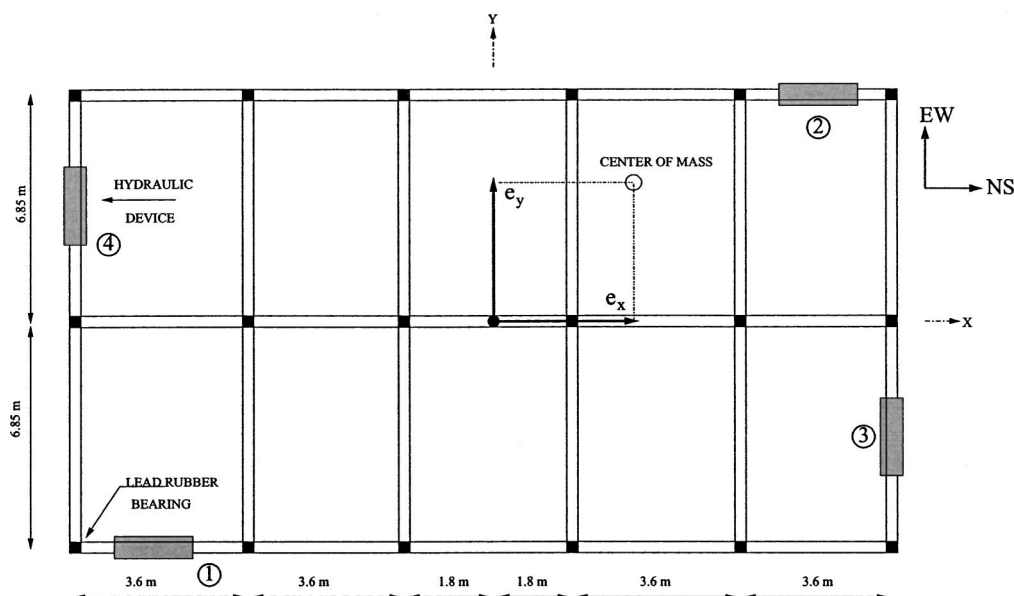


Fig. 5. Six-story structure: Plan

Table 1. Comparison of Response of Base Isolation System and Semiactive Device for El Centro

Response		Lead rubber bearings		Lead rubber bearings with semiactive viscous damping		Lead rubber bearings with supplemental viscous damping	
		$e = 0$ m	$e = 5.64$ m	$e = 0$ m	$e = 5.64$ m	$e = 0$ m	$e = 5.64$ m
Max. base disp. (m)	N-S	0.081	0.091	0.046	0.036	0.060	0.052
	E-W	0.073	0.073	0.043	0.046	0.062	0.062
Max. base shear (t)	N-S	359	327	352	335	342	325
	E-W	305	267	325	269	254	227
Max. base rotation	—	0.00084	0.01038	0.00121	0.00407	0.00187	0.00451
Max. Z moment (t m)	—	573	1,585	1,274	2,017	1,107	1,638

stant c_v is defined as $c_v = c_v^* A_p^2$. Here, f , k_d , and c_v are the force, stiffness, and damping in the device, respectively, and $c_v(v)$ is the only term that can be controlled, by the valve-opening variable v . This valve coefficient $c_v(v)$ is assumed to vary linearly with the valve variable v

$$c_v(v) = (1-v)c_{\min} + vc_{\max} \quad (11)$$

The constants c_{\min} and c_{\max} are the damping coefficients when the device is “OFF” and “ON”, respectively, and, the valve is modeled using a first-order differential equation

$$\dot{v} = \frac{1}{T_v}(u-v) \quad (12)$$

where T_v =valve time constant and u =control input which depends on the control rule. For the particular control rule considered in this study u is bounded by $0 \leq u \leq 1$ and is given by

$$u = H(f \cdot V_a) \quad (13)$$

where V_a =absolute velocity of the structure side of the device with respect to an inertial reference frame and $H(\cdot)$ =Heaviside step function. Force may be measured with a load cell or with pressure transducers on the cylinder.

Appropriate values for the device parameters c_{\min} , c_{\max} and k_d are determined through iterative time history analyses of the semiactive isolation system. To design the cylinder and piston arrangement one specifies a suitable bore diameter D_b , rod diameter D_r , piston stroke S , and fluid volume V_T . The area of the piston is determined by the force requirement F_{\max} .

Extension to 3DBASIS

The program 3DBASIS (Nagarajaiah et al. 1989) computes the nonlinear dynamic response of three-dimensional base-isolated structures. Buildings modeled by 3DBASIS have three degrees of freedom per story: two horizontal translations and one rotation. Models for a number of isolator types, including elastomeric bearings and sliding isolation bearings with recentering properties are implemented in this program and can be combined to model a complete isolation system. Additionally, the program takes into account the lateral-torsional interaction of forces in both horizontal directions, and the biaxial hysteretic behavior of each individual isolator.

In this study we implement a semiactive hydraulic device in parallel with a hysteretic lead-rubber bearing isolation system. The device is modeled as an additional new isolation element. A fourth-order Runge-Kutta method (Butcher 1987) is employed to solve the first-order differential equations for the isolators and the semiactive device, which are given by Eqs. (9) and (12).

Simulations

In this section, we present the simulation results for a typical structure subjected to different earthquake input motions. Response of the same structure with three different types of base-isolation systems, namely, lead rubber bearings, lead rubber bearings with supplemental viscous damping, and lead rubber bearings with semiactive viscous damping.

Description of Model

A six-story reinforced concrete structure as shown in Figs. 1 and 5 is considered for the purposes of the simulations. This structure is similar to the one studied by Nagarajaiah et al. (1989). The total weight of the structure is 2,205 tons. The fixed-base frequencies of the structure for the first three modes are 1.147, 1.202, and 2.503 Hz. The rigid body isolation period (T_b) is 1.65 s. Damping of 5% of critical is assumed for the superstructure in all the modes.

In the lead rubber bearing isolation system model, the post-yielding to preyielding stiffness ratio is 0.154, the yield force is 75.8 kN and the yield displacement is 7.00 mm.

Four hydraulic devices, two in each of the orthogonal directions as shown in Fig. 5, are installed in parallel with 18 lead rubber bearings, which are placed under the columns. The stiffness k_d of the hydraulic devices are 300 kN/mm and c_{\max} and c_{\min} are 3 kN/mm/s and 300 N/mm/s, respectively. The relative mistiming of the semiactive devices is given by dimensionless quantities α and β , where α is the ratio between the time constants of the devices in the north-south (NS) direction, given by T_1/T_2 , and β is the ratio between the time constants of the devices in the east-west (EW) direction, given by T_3/T_4 , and where T_1 , T_2 , T_3 , and T_4 are the time constants of device 1, 2, 3, and 4, respectively. The time constants T_2 and T_4 are fixed at 0.010 s. The response of the structure is simulated for values of α and β equal to 1, 2, 5, and 10. The value of 10 is extremely high, however, it is used on purpose to represent the case where one of the devices totally fails in one direction, while the other one functions properly. Results corresponding to variations in α are given in this paper. Results corresponding to variations in β are qualitatively similar to the results corresponding to variations in α (Oka 2000).

Earthquake Data

The three models mentioned above were each subjected to three different earthquake input motions in both the orthogonal directions:

1. The May 18, 1940 Imperial Valley earthquake recorded at the El Centro site. The peak acceleration in NS and EW directions are 0.34 and 0.21 g respectively;

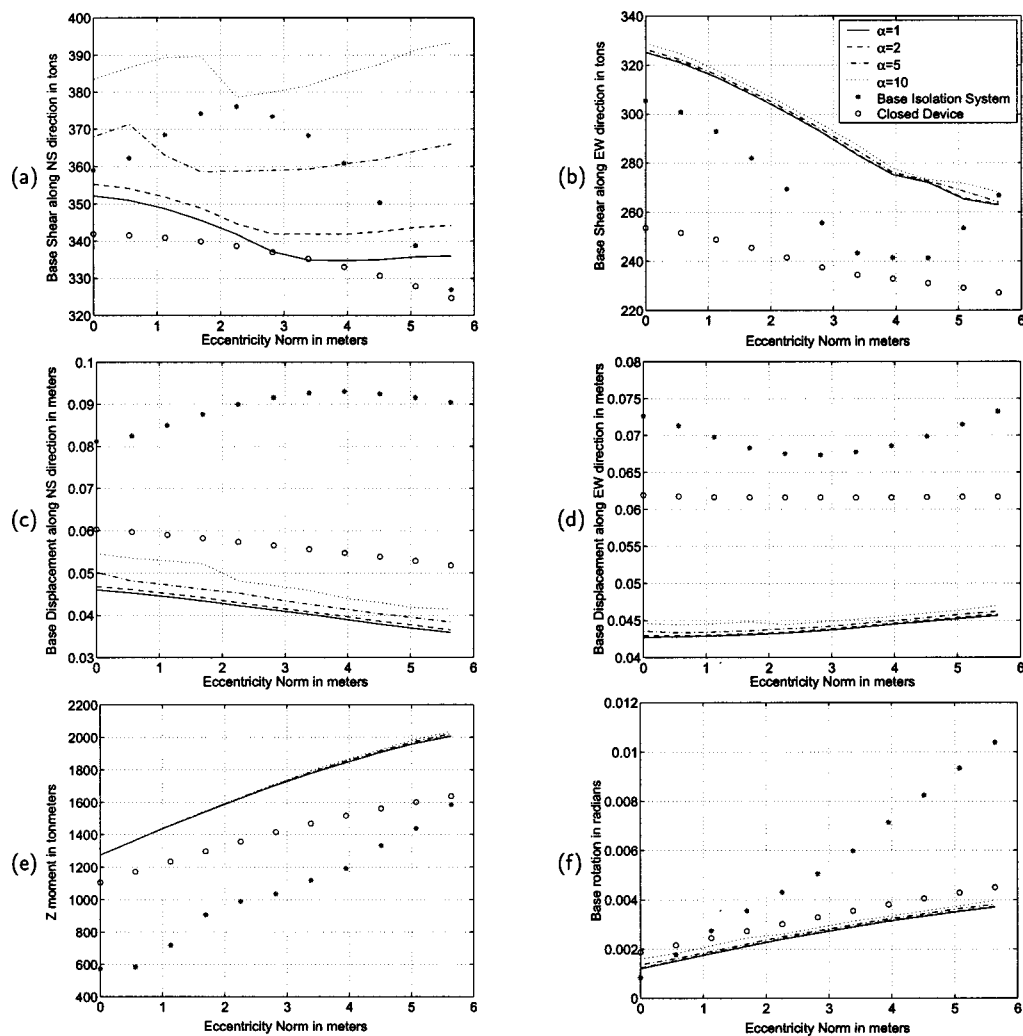


Fig. 6. Comparison of isolation drift (a) and (b), base shears (c) and (d), torsional rotation and moment (e) and (f) between LRB system, LRB-SAVD system with variation in α , and LRB-VD system for El Centro

2. The October 15, 1979 Imperial Valley earthquake recorded at the Meloland station. The peak acceleration in NS and EW directions are 0.31 and 0.29 g respectively; and
3. The January 17, 1994 Northridge earthquake recorded at the Sylmar Hospital free field station. The peak acceleration in NS and EW directions are 0.8 and 0.6 g respectively.

Eccentricity Norm

In order to quantify the mass eccentricity of the structure we define an eccentricity norm as

$$e = \sqrt{(e_x^2 + e_y^2)} \quad (14)$$

Table 2. Comparison of Response of Base Isolation System and Semiactive Device for Meloland

Response		Lead rubber bearings		Lead rubber bearings with semiactive viscous damping		Lead rubber bearings with viscous damping	
		$e = 0$ m	$e = 5.64$ m	$e = 0$ m	$e = 5.64$ m	$e = 0$ m	$e = 5.64$ m
Max. base disp. (m)	N-S	0.213	0.211	0.085	0.081	0.103	0.150
	E-W	0.383	0.273	0.129	0.114	0.092	0.129
Max. base shear (t)	N-S	683	718	535	480	486	453
	E-W	1271	846	684	596	732	599
Max. base rotation	—	0.00324	0.04295	0.00468	0.00991	0.00546	0.01191
Max. Z moment (t m)	—	840	4,767	1,308	2,017	1,447	2,463

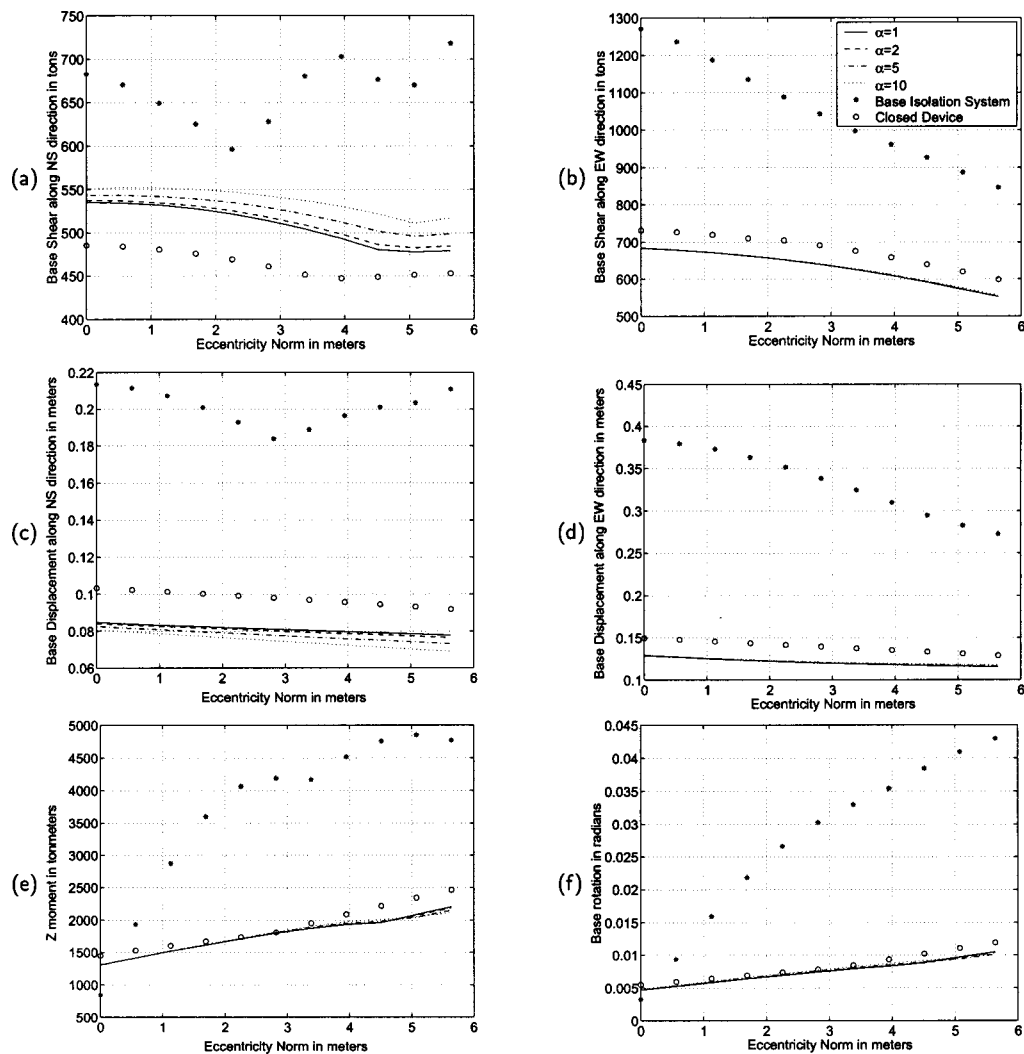


Fig. 7. Comparison of isolation drift (a) and (b), base shears (c) and (d), torsional rotation and moment (e) and (f) between LRB system, LRB-SAVD system with variation in α , and LRB-VD system for Meloland

where e_x and e_y = mass eccentricities of the superstructure in the X and Y direction with respect to the center of mass of the base. This eccentricity should not be confused with the eccentricity between the center of mass and center of stiffness in the superstructure itself. Note that the center of masses do not coincide with the center of stiffnesses of the respective stories in the superstructure that we studied and therefore there is an inherent eccentricity in the superstructure itself, which results in some tor-

sional response even when the superstructure center of mass coincides with the base center of mass, i.e. $e = 0.0$.

The response of the structure is simulated with different eccentricity norms. The eccentricities in both the orthogonal directions are varied from zero to one-fourth of the length of the structure in each respective direction. For this model problem e_x and e_y were varied from 0 to 4.5 m and 0 to 3.4 m, respectively.

Table 3. Comparison of Response of System and Device for Sylmar

Response		Lead rubber bearings		Lead rubber bearings with semiactive viscous damping		Lead rubber bearings with viscous damping	
		$e = 0$ m	$e = 5.64$ m	$e = 0$ m	$e = 5.64$ m	$e = 0$ m	$e = 5.64$ m
Max. base disp.	N-S	0.528	0.334	0.233	0.224	0.249	0.241
(m)	E-W	0.441	0.281	0.132	0.126	0.143	0.135
Max. base shear	N-S	1650	1404	1087	1082	1097	1100
(t)	E-W	1117	918	713	656	686	596
Max. base rotation	—	0.00335	0.01721	0.00275	0.00615	0.00289	0.00486
Max. Z moment	—	825	3,266	2,130	3,810	2,189	3,660
(t m)							

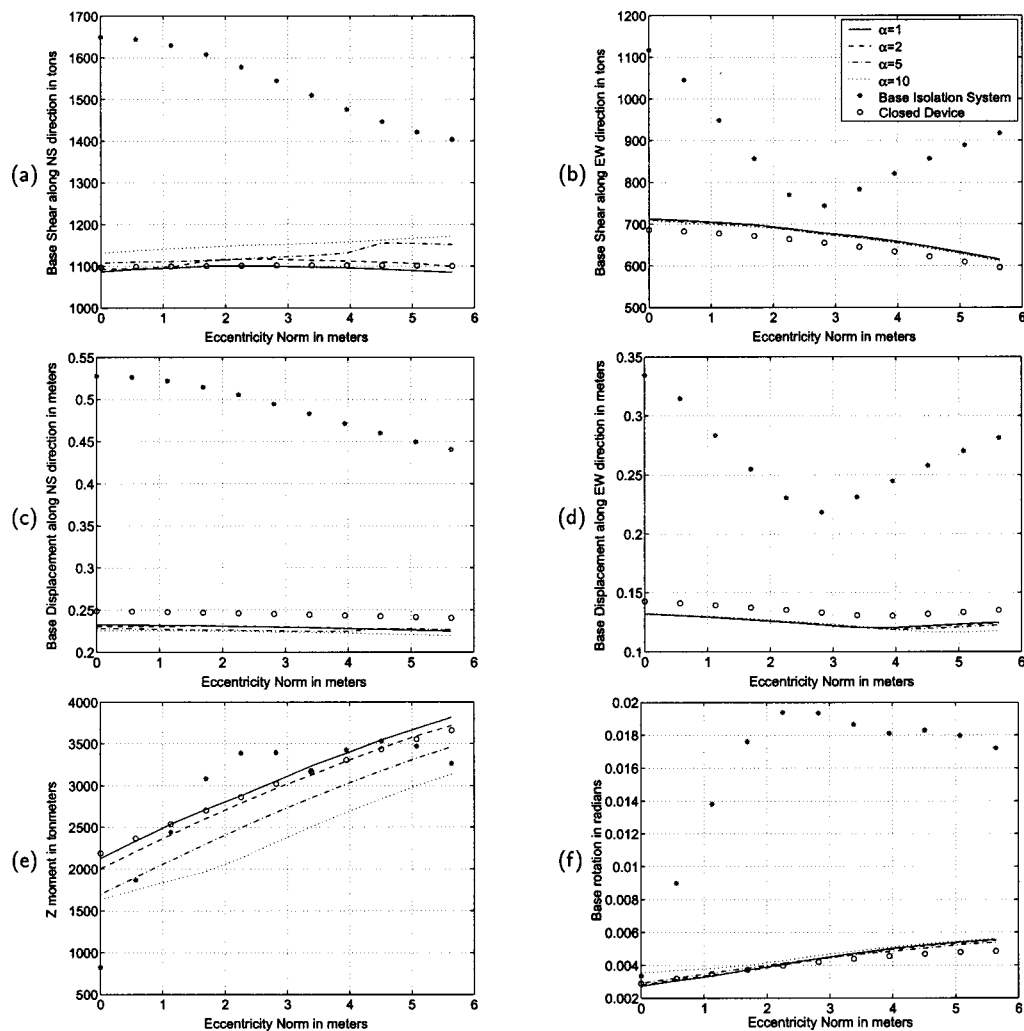


Fig. 8. Comparison of isolation drift (a) and (b), base shears (c) and (d), torsional rotation and moment (e) and (f) between LRB system, LRB-SAVD system with variation in α , and LRB-VD system for Sylmar

Results

The objective of controlling the isolation damping is to substantially reduce the isolator drift without increasing the base shear. Peak isolation drift, peak base shear, peak base rotation, and peak torsional moment are plotted against the eccentricity norm for all three systems: The base isolation system (lead rubber bearings only) and the systems with the semiactive hydraulic devices (the controlled valve and the closed valve cases) for each earthquake.

El Centro Record of 1940 Imperial Valley Earthquake

Table 1 and Fig. 6 show that for the El Centro ground motions, the LRB-SAVD system results in isolation drifts and rotations that are 20 to 40% smaller than both the LRB and LRB-VD cases. The LRB-SAVD system does not increase the base shear in the NS direction but increases the base shear by 5 to 30% in the EW direction. However, the maximum torsional moment for both the LRB-SAVD and LRB-VD increases by about 500–700 t-m as compared to the LRB system. The eccentricity does not have a significant effect on the isolation drift, base shear, or the base rotation for the system with the semiactive device. However, the torsional moments increase by 60% (800 t-m) as the eccentricity

increases. The effect of the time lag is significant only in the base shear response in the NS direction.

Meloland Record of 1979 Imperial Valley Earthquake

Table 2 and Fig. 7 show that the LRB-SAVD system reduces the isolation drift by 55% (12 cm) in the NS direction and 60% (16 cm) in the EW direction as compared to the LRB system, and by 20% (2 cm) in the NS direction and 10% (2 cm) in the EW direction as compared to the LRB-VD system. The LRB-SAVD system reduces the base shear by 20% in the NS direction and 35 to 45% (200 to 550 t) in the EW direction as compared to the LRB system. As compared to the LRB-VD system, the LRB-SAVD system increases the base shear by 15% (60 t) in the NS direction but decreases it by 9% (60 t) in the EW direction.

In regard to the torsional moments and rotations, the LRB-SAVD and LRB-VD systems behave almost identically. The torsional response increases monotonically with mass eccentricity, while the isolation drift and base shear in the EW direction decrease monotonically with the mass eccentricity. The LRB system is much more sensitive to the mass eccentricity than the LRB-SAVD and LRB-VD systems. As in the El Centro response, the effect of time lag is not pronounced.

Sylmar Record of 1994 Northridge Earthquake

Table 3 and Fig. 8 show that the LRB-SAVD system reduces the isolation drift by 50 to 60% (23 to 31 cm in the NS direction and by 40 to 60% in the EW direction as compared to the LRB system. As compared to the LRB-VD system, the LRB-SAVD system reduces the isolation drift by 10% (2 cm).

The base shear for the LRB-SAVD and the LRB-VD systems are essentially the same, and are 20 to 30% (300 to 550 t) smaller than those for the LRB system in the NS direction. In the EW direction, the LRB-SAVD and LRB-VD systems reduce the base shear by 10 to 35% (70 to 400 t). The torsional moments for all these systems are essentially the same, whereas the torsional rotation for the LRB-SAVD and LRB-VD systems are 70% smaller than those of the LRB system. Again, the torsional response increases monotonically with the mass eccentricity. The NS response for the LRB case decreases monotonically with the mass eccentricity. The effect of time lag in the LRB-SAVD system is insignificant except for the torsional moment.

For each of the three earthquakes it is observed that unmatched time lags do not appear to degrade the system behavior. Also, the response of the structure installed with semiactive devices seems to be more or less constant with increases in the mass eccentricity.

It is interesting to note that the benefits of the LRB-SAVD system are clearer for the Meloland and Sylmar records than for the El Centro record. The basic difference between these two earthquakes and El Centro is that they contain a large velocity pulse. Thus, the semiactive damping system described in this paper appears to be well suited to earthquakes that have a large velocity pulse.

Dimensions of Hydraulic Device

We design the hydraulic device using the maximum force in the device F_{\max} , maximum displacement of the device D_{\max} , and maximum velocity of the device V_{\max} as computed in the dynamic simulations, in which c_{\max} and c_{\min} are 3 kN/mm/s and 300 N/mm/s, respectively. F_{\max} , V_{\max} , and D_{\max} are calculated as 92.71, 235.7, 375.2 t; 0.25, 0.60, 1.1 m/s; and 5.4, 16.94, 24.67 cm for El Centro, Meloland, and Sylmar earthquake records, respectively. For a F_{\max} range of 90 to 375 t, a D_{\max} range of 5 to 25 cm and a maximum velocity range of 0.25 to 1.1 m/s and assuming a maximum fluid pressure of 3.6 kN/cm², a device with a rod diameter of 18.5 cm bore diameter of 40.5 cm and a stroke of 0.5 m is found to provide the target stiffness, k_d , of 300,000 kN/m that was used in the analysis. Equivalently, several smaller devices may be implemented in parallel.

Conclusions

A nonlinear dynamic analysis of a structure fitted with a semiactive hydraulic device was performed using the 3DBASIS program. The analysis was carried out with three different earthquake records. The results showed that semiactive hydraulic devices are capable of controlling the response of the structure especially in case of earthquake ground motions with a large velocity pulse. The semiactive hydraulic device performs better than the conventional base-isolated system especially for the earthquakes with large pulses.

In the case of the moderate El Centro earthquake, there was a moderate increase in the base shear and the torsional moment in

the system where semiactive devices are used as compared to the system where conventional base isolation is used.

For all the earthquakes, as the mass eccentricity increases, both the torsional moment and the base rotation, increase. However, mismatched time lags in the devices do not cause a significant increase in the torsional response. Semiactive control systems appear to be robust to relative time lags between the devices. Even for the worst cases considered, where the ratio of the time constants between the devices in the same direction was ten, there was no significant increase due to the time lag, either in the torsional moments and base rotations, or in the base shear and isolation drifts.

Acknowledgments

This material is based on work supported by the National Science Foundation under Award No. CMS-9900193. Any opinions, findings, and conclusions or recommendations expressed in this publication are those of the writers and do not necessarily reflect the views of the sponsors. The writers thank the reviewers for their helpful comments.

References

- Akbay, Z., and Aktan, H. M. (1990), "Intelligent energy dissipation devices." *Proc., 4th U.S. National Conf. on Earthquake Engineering*, Palm Springs, Calif., Vol. 3, 427–435.
- Butcher, J. C. (1987), *The numerical analysis of ordinary differential equations*, Wiley, New York.
- Carlson, J. D., and Spencer, B. F., Jr. (1996), "Magnetorheological fluid dampers for semi-active seismic protection." *Proc., 3rd Int. Conf. on Motion and Vibration Control*, Chiba, Japan, Vol. 3, 35–40.
- Dowdell, D. J., and Cherry, S. (1994), "Structural control using semi-active friction dampers." *Proc., 1st World Conf. on Structural Control*, International Association for Structural Control, Los Angeles, Vol. 3, FA1-59-FA1-68.
- Dynamic Isolation Systems (DIS). (2001). "Kobe earthquake: Effectiveness of seismic isolation proven again." (<http://www.dis-inc.com>).
- Environmental Engineering Research Co. (EERC). (2001). "Seismically-isolated buildings in the United States." UC Berkeley, (<http://nisee.berkeley.edu/prosys/usblbds.html>).
- Ehrgott, R. C., and Masri, F. (1993). "Structural control applications of an electrorheological device." *Proc., Int. Workshop on Structural Control*, Honolulu, 115–129.
- Feng, M. Q. (1993). "Application of hybrid sliding isolation system to buildings." *J. Eng. Mech.*, 119(10), 2090–2108.
- Gavin, H. P. (2001). "Control of seismically excited vibration using electrorheological materials and Lyapunov methods." *IEEE Trans. Control Syst. Technol.*, 9(1), 27–36.
- Gavin, H. P., and Doke, N. S. (1999). "Resonance suppression through variable stiffness and damping mechanisms." *Proc., SPIE, 6th Annual Int. Symp. on Smart Structures and Materials*, Newport Beach, Calif., 43–53.
- Gavin, H. P., and Hanson, R. D. (1998). "Seismic protection using ER damping walls." *Proc., 2nd World Conf. on Structural Control*, Kyoto, Japan, Vol. 2, Wiley, 1183–1188.
- Gavin, H. P., Hanson, R. D., and McClamroch, N. H. (1996). "Control of structures using electrorheological dampers." *Proc., 11th World Conf. on Earthquake Engineering*, Acapulco, Mexico, Pergamon, CD-ROM Proceedings.
- Gavin, H. P., Morales, R., and Reilly, K. (1998). "Drift-free integrators." *Rev. Sci. Instrum.*, 69(5), 2171–2175.
- Heaton, T. H., Hall, J. F., Wald, D. J., and Halling, M. W. (1995). "Response of high-rise and base-isolated buildings to a hypothetical M_w 7.0 blind trust earthquake." *Science (Washington, DC, U.S.)*, 267, 206–211.

- Hirai, J., Naruse, M., and Abiru, H. (1996). "Structural control with variable friction damper for seismic response." *Proc. 11th World Conf. on Earthquake Engineering*, Acapulco, Mexico, Pergamon, CD-ROM Proceedings.
- Housner, G. W., Bergman, L. A., Caughey, T. K., Chassiakos, A. G., Claus, R. O., Masri, S. F., Skelton, R. E., Soong, T. T., Spencer, B. F., and Yao, J. T. P. (1997). "Structural control: Past, present and future." *J. Eng. Mech.*, 123(9), 897–971.
- Hussain, S. M., and Retamal, E. (1994). "A hybrid seismic isolation system—isolators with supplemental viscous dampers." *Proc., 1st World Conf. on Structural Control*, Los Angeles, Vol. 3, FA2-53–FA2-62.
- Jangid, R. S., and Datta, T. K. (1992). "Seismic behavior of torsionally coupled base isolated structure." *Eur. Earthquake Eng.*, 3(92), 2–13.
- Jangid, R. S., and Datta, T. K. (1993). "Seismic response of a torsionally coupled system with a sliding support." *J. Struct. Build. Inst. Civ. Eng.*, 99, 271–280.
- Jangid, R. S., and Datta, T. K. (1994). "Nonlinear response of torsionally coupled base isolated structure." *J. Struct. Eng.*, 120(1), 1–22.
- Jangid, R. S., and Datta, T. K. (1995). "Performance of base isolation systems for asymmetric building subject to random excitation." *Eng. Struct.*, 17(6), 443–454.
- Johnson, E. A., Ramallo, J. C., Spencer, B. F., and Sain, M. K. (1998). "Intelligent base isolation systems." *Proc., 2nd World Conf. on Structural Control*, Kyoto, Japan, Wiley, Vol. 1, 367–376.
- Karnopp, D. (1990). "Design principles for vibration control systems using semi-active dampers." *ASME J. Dyn. Syst. Meas. Control*, 112(3), 448–455.
- Karnopp, D., and Allen, R. (1975). "Semi-active control of multi-mode vibratory systems using the ILSM concept." *ASME J. Eng. Ind.*, 98(3), 914–918.
- Karnopp, D., Crosby, M. J., and Harwood, R. A. (1974). "Vibration control using semi-active force generators." *ASME J. Eng. Ind.*, 96(2), 619–626.
- Kelly, J. M. (1991). "Base isolation: origins and development." (<http://nisee.berkeley.edu/lessons/kelly.html>).
- Kelly, J. M. (1997). *Earthquake-resistant design with rubber*, 2nd Ed., Springer-Verlag, Berlin.
- Kelly, J. M. (1999). "The role of damping in seismic isolation." *Earthquake Eng. Struct. Dyn.*, 28, 3–20.
- Khalil, H. K. (1996). *Nonlinear systems*, 2nd Ed., Prentice-Hall, Englewood Cliffs, N.J.
- Kurata, N., Kobori, T., Takahashi, M., Niwa, N., and Midorikawa, H. (1999). "Actual seismic response controlled building with semi-active damper system." *Earthquake Eng. Struct. Dyn.*, 28, 1427–1447.
- Lee, D. M. (1980). "Base isolation for torsion reduction in asymmetric structures under earthquake loading." *Earthquake Eng. Struct. Dyn.*, 8(4), 349–359.
- Makris, N., Hills, D., Burton, S., and Jordan, M. (1995). "Electrorheological fluid dampers for seismic protection of structures." *Proc. SPIE Conf. on Smart Structures and Materials*, San Diego, 184–194.
- McGreevy, S., Soong, T. T., and Reinhorn, A. M., (1988). "An experimental study of time delay compensation in active structural control." *Proc. 6th Int. Modal Analysis Conf.*, Orlando, Fla., Vol. 1, 733–739.
- Meirovitch, L., and Stemple, T. J. (1997). "Nonlinear control of structures in earthquakes." *J. Eng. Mech.*, 123(10), 1090–1095.
- Moroni, M. O., Sarrazin, M., and Boroschek, R. (1998). "Experiments on a base-isolated building in Santiago, Chile." *Eng. Struct.*, 20(8), 720–725.
- Naeim, F., and Kelly, J. M. (1999). *Design of seismic isolated structures: From theory to practice*, Wiley, New York.
- Nagarajaiah, S., and Ferrell, K. (1999). "Stability of elastomeric seismic isolation bearings." *J. Struct. Eng.*, 125(9), 946–954.
- Nagarajaiah, S., Reinhorn, A. M., and Constantinou, M. C. (1991). "Non-linear dynamic analysis of 3-D-base-isolated structures." *J. Struct. Eng.*, 117(7), 2035–2054.
- Nagarajaiah, S., Reinhorn, A. M., and Constantinou, M. C. (1992). "Experimental study of sliding isolated structures with uplift restraint." *J. Struct. Eng.*, 118(6), 1666–1682.
- Nagarajaiah, S., Reinhorn, A. M., and Constantinou, M. C. (1993). "Torsional coupling in sliding base-isolated structures." *J. Struct. Eng.*, 119(1), 130–149.
- Nagarajaiah, S., Reinhorn, A. M., and Constantinou, M. C. (1989). "Non-linear dynamic analysis of three-dimensional base isolated structures (3d-basis)." *Technical Rep. NCEER-89-0019*, National Center of Earthquake Engineering Research, State Univ. of New York, Buffalo, New York.
- Nagarajaiah, S., and Xiahong, S. (2000). "Response of base-isolated USC hospital building in Northridge earthquake." *J. Struct. Eng.*, 126(10), 1177–1186.
- Oka, N. A. (2000). "Nonlinear dynamic analysis of an asymmetric structure fitted with semi-active hydraulic devices." MSc thesis, Duke Univ., Durham, N.C.
- Onoda, J., Oh, H. U., Minesugi, K. (1997). "Semi-active vibration suppression of truss structures by electrorheological fluid." *Acta Astron.*, 40(11), 771–779.
- Pan, T. C., and Kelly, J. M. (1983). "Seismic response of torsionally coupled base isolated building." *Earthquake Eng. Struct. Dyn.*, 11, 749–770.
- Patten, W. N., Mo, C., Kuehn, M. J., and Lee, J. (1998). "A primer on design of semi-active vibration absorbers." *J. Eng. Mech.*, 124(1), 61–68.
- Skinner, R. I., Robinson, W. H., and McVerry, G. H. (1993). *An introduction to seismic isolation*, Wiley, New York.
- Soong, T. T. (1990). *Active structural control: Theory and practice*, Longmans Green, New York.
- Spencer, B. F., Jr., Dyke, S. J., and Sain, M. K. (1996). "Magnetorheological dampers: A new approach to seismic protection of structures." *Proc. IEEE Conf. on Decision and Control*, Chiba, Japan, 3.
- Spencer, B. F., Jr., and Sain, M. K. (1997). "Controlling buildings: A new frontier in feedback." *IEEE Control Systems Magazine: Special Issue on Emerging Technologies*, 17(6), 19–35.
- Symans, M. D., and Constantinou, M. C. (1997a). "Seismic testing of a building structure with a semiactive fluid damper control system." *Earthquake Eng. Struct. Dyn.*, 26, 759–777.
- Symans, M. D., and Constantinou, M. C. (1997b). "Experimental testing and analytical modeling of semi-active fluid dampers for seismic protection." *J. Intell. Mater. Syst. Struct.*, 8(8), 644–657.
- Symans, M. D., and Constantinou, M. C. (1999). "Semi-active control systems for seismic protection of structures: A state of the art view." *Eng. Struct.*, 21(6), 469–487.
- Tyler, R. G. (1977). "Dynamic tests on PTFE sliding layers under earthquake conditions." *Bull. New Zealand Nat. Soc. Earthquake Eng.*, 10(3), 129–138.
- Wang, Y. P., Chung, L. L., and Liao, W. H. (1998). "Seismic response analysis of bridges isolated with friction pendulum bearings." *Earthquake Eng. Struct. Dyn.*, 27, 1069–1093.
- Yang, J. N., Kim, J. H., and Agrawal, A. K. (2000). "Resetting semiactive stiffness damper for seismic response control." *J. Struct. Eng.*, 126(12), 1427–1433.